inorganics

MDPI

Article

Temperature-Sensitive Chameleon Luminescent Films Based on PMMA Doped with Europium(III) and Terbium(III) Anisometric Complexes

Yuriy G. Galyametdinov [1,2], Aleksandr S. Krupin [1] and Andrey A. Knyazev [1,*]

[1] Department of Physical and Colloid Chemistry, Kazan National Research Technological University, 68 Karl Marx Street, 420015 Kazan, Russia; yugal2002@mail.ru (Y.G.G.); krupin_91@mail.ru (A.S.K.)
[2] Zavoisky Physical-Technical Institute, FRC Kazan Scientific Center of RAS, 10/7 Sibirsky Tract, 420029 Kazan, Russia
* Correspondence: knjazev2001@mail.ru

Abstract: The spin-coating technique was used to produce composite films consisting of PMMA polymer doped with anisometric complexes of Eu(III) and Tb(III). It was found that an increase in the content of Tb^{3+} complexes intensifies emission of both ions due to the intermolecular energy transfer from the Tb(III) complex to the Eu(III) complex, which results in the increase in the relative luminescence quantum yield of Eu(III) ion by 36%. The temperature sensitivity of the film luminescence intensity and lifetime in the range of 296–363 K was investigated. The maximum relative sensitivity of the films reaches 5.44% × K^{-1} and exceeds that of all known lanthanide-containing thermal sensors designed for measuring physiological temperatures. In combination with changing luminescence color, such a sensitivity makes these films promising colorimetric thermal sensors for in situ temperature measurements.

Keywords: Ln(III) complexes; PMMA; photoluminescence; thermometry

check for updates

Citation: Galyametdinov, Y.G.; Krupin, A.S.; Knyazev, A.A. Temperature-Sensitive Chameleon Luminescent Films Based on PMMA Doped with Europium(III) and Terbium(III) Anisometric Complexes. *Inorganics* **2022**, *10*, 94. https://doi.org/10.3390/inorganics10070094

Academic Editor: Valentina Utochnikova

Received: 28 May 2022
Accepted: 29 June 2022
Published: 4 July 2022

Publisher's Note: MDPI stays neutral with regard to jurisdictional claims in published maps and institutional affiliations.

Copyright: © 2022 by the authors. Licensee MDPI, Basel, Switzerland. This article is an open access article distributed under the terms and conditions of the Creative Commons Attribution (CC BY) license (https://creativecommons.org/licenses/by/4.0/).

1. Introduction

Luminescent thermometry is an emerging technology that can be used in microelectronics, photonics, microfluidics, medicine and biology [1–5]. Compared to other electronic thermal sensor techniques, the advantages of luminescent thermometry are its ability to monitor surface temperatures with micro- and nanometer-scale spatial resolution (<10 μm), high sensitivity (>1% × K^{-1}), fast response (<1 ms) and measurement accuracy, small size of sensitive elements and resistance to electromagnetic interference [2,6]. The working principle of luminescent thermometers is monitoring the effect of temperature on the luminescence parameters: quenching time, intensity, emission peak area or position and the ratio of intensities of emission bands [7]. Several types of luminophores are already used as temperature sensors, including organic compounds, quantum dots, metal clusters, dye-doped nanoparticles, metal-ligand complexes and lanthanide-containing materials [8,9]. Narrow emission bands of lanthanides make it possible to measure temperature changes with high accuracy. In addition to these properties, lanthanides have a long luminescence lifetime and allow for using temporal methods for increasing signal-to-noise ratios [10]. Materials with two different lanthanide ions are attractive components of ratiometric thermometers [11,12]. Such materials are characterized by high accuracy, photostability and temporal resolution of signals. The accuracy of temperature measurements by an absolute emission intensity is sensitive to external factors such as an excitation power and errors in opto-electronic systems. On the other hand, the luminescence intensity ratio of two luminophores is almost constant, so no additional calibration of a thermal probe is needed for such a double system [13,14].

Among lanthanide coordination compounds, β-diketonate complexes are the most promising materials due to their luminescence with high quantum yield (up to 85% [15,16]),

large Stokes shifts, decay time of luminescence in the range of tens to hundreds of microseconds and high temperature sensitivity of luminescence intensity (>1% × K^{-1}) [17]. They also possess a set of attractive chemical properties: a relatively easy synthesis, a good solubility in a wide range of common solvents and an ability to be incorporated into various matrices [18–20].

In recent years, the focus of studies in this area is shifting more and more from synthesis of coordination lanthanide compounds to their inclusion into various types of matrices (inorganic, organic or organic-inorganic). A matrix is noticed to enhance not only thermal and chemical stability of complexes and their mechanical strength [21,22] but luminescence efficiency as well [23,24]. Two principal approaches are considered in this aspect: encapsulation of a lanthanide complex into polymer [25–27] and synthesis of lanthanide-containing polymers [28,29]. Polymers are ideal candidates for matrices as they possess attractive technological properties such as flexibility, processability, mechanical strength and low cost.

However, to control the distribution of temperature over a surface, we need film materials with intensive luminescence that are transparent in the visible range. The majority of currently known lanthanide(III) β-diketonate complexes have a crystalline structure, so it is difficult to use them for producing homogeneous films. It is necessary to use hard UV radiation for their excitation [30], which makes the resulting thermal sensors expensive and reduces their photostability.

In this work, we examined the possibility of making thermosensitive films using PMMA polymer and anisometric Tb(III) and Eu(III) complexes. The presence of long hydrocarbon substituents at the ends of molecules makes such compounds amorphous, which allows them to form transparent media with no crystalline defects. Good solubility of such complexes in organic solvents and miscibility with polymers [31,32] ensure their uniform dispersal in the film material. Additionally, they absorb light effectively in a wide range from 250 to 400 nm, which eliminates the need to use hard UV radiation for their excitation [33–35]. In addition to the advantages listed above, the use of multi-ion lanthanide complexes should enhance an intermolecular energy transfer, according to known theoretical prerequisites and experimental data, thus increasing the efficiency of a thermal sensor [36,37].

2. Results and Discussion

The original 1,10-phenanthroline and β-diketone were used as the ligands for the synthesis of the complexes. The triplet levels of these compounds provide an effective energy transfer to the emitting levels of Eu^{3+} and Tb^{3+} ions (Figure 1). Their composition and structure were confirmed by mass spectrometry and elemental analysis.

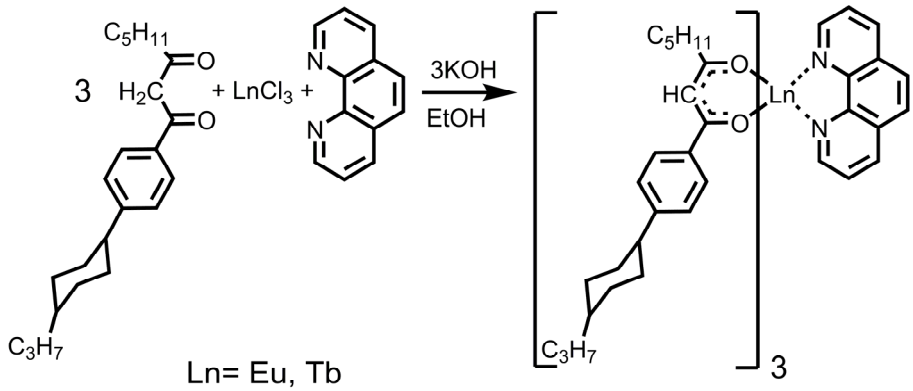

Figure 1. Synthesis of Ln(III) compounds.

These complexes are amorphous powders that are soluble in organic non-polar and weakly polar solvents. They are mutually miscible as well as miscible with PMMA polymer [31,38].

A spin-coating process was used to produce composite films of PMMA polymer doped with 3 w.% of the Eu(III) compound and 1–20% w.% of the Tb(III) compound (3%EuX%Tb) [39]. The films are 300 nm thick (±10%). The films are almost transparent in the infrared and visible ranges (transmittance over 90%), whereas they absorb light strongly in the UV range (Figure S1).

UV irradiation of the PMMA films doped with the individual Tb(III) and Eu(III) ions results in luminescence that is typical for the respective Ln(III) ions (Figure 2).

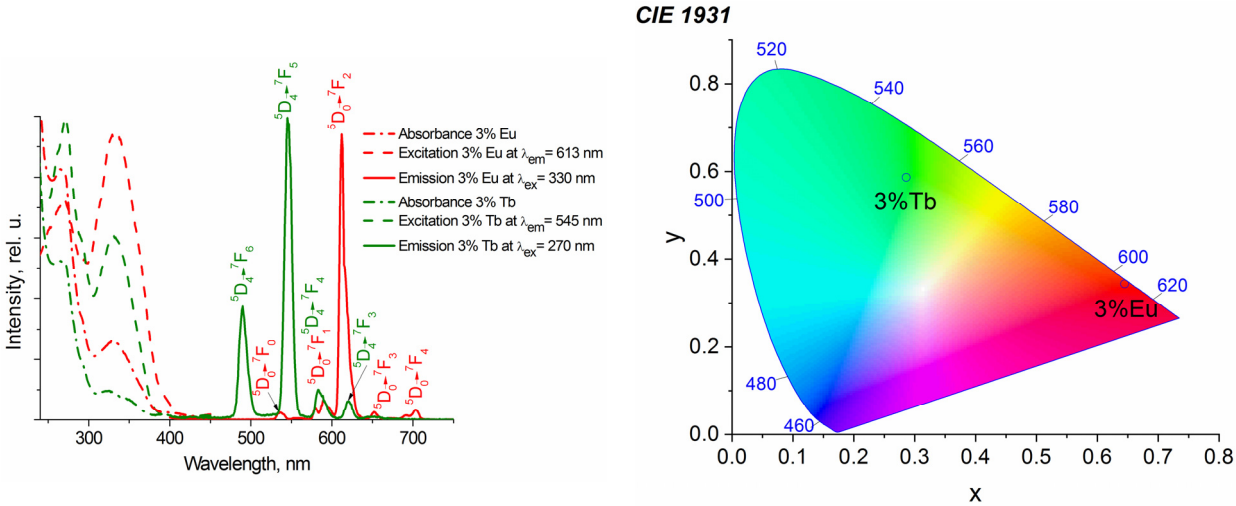

(**a**) (**b**)

Figure 2. Luminescence and absorption spectra (**a**) and the CIE diagram (**b**) of PMMA films with 3 w.% of Tb(III) and Eu(III) complexes.

An increase in the content of the Tb(III) complexes in the 3%EuX%Tb films intensifies emission of both the Tb^{3+} and Eu^{3+} ions due to occurring intermolecular energy transfer (Figure 3). Because of large distances between ions, the most probable energy transfer mechanism is a dipole–dipole interaction (Förster) rather than an exchange energy transfer (Dexter).

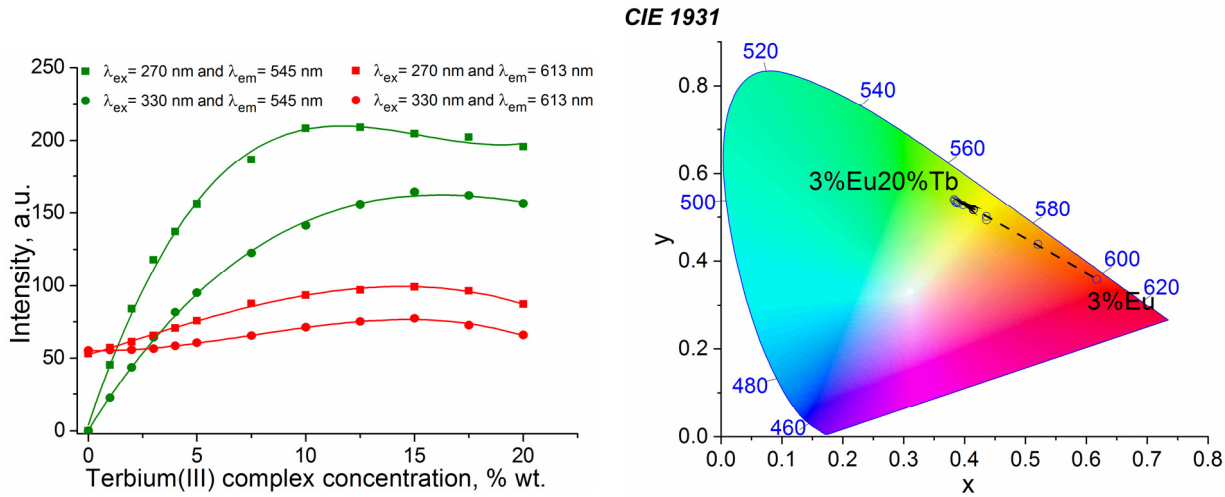

(**a**) (**b**)

Figure 3. Concentration dependences of luminescence (**a**) obtained for the 3%EuX%Tb at λ_{ex} = 270 and 330 nm and λ_{em} = 545 and 613 nm; the CIE diagram (λ_{ex} = 330 nm) (**b**).

It was demonstrated that the emission intensity at λ_{em} = 613 nm of the 3%Eu15%Tb film increases by 2 times at λ_{ex} = 270 nm and by 1.4 times at λ_{ex} = 330 nm, respectively, as compared with the film of the individual Eu(III) compound in PMMA (3%Eu).

The overall luminescence quantum yield of the complex upon excitation of the chromophore is determined by the efficiency of the sensitization (η_{sens}) and by the emission quantum efficiency (φ^{Ln}) of the lanthanide luminescence (Equation (1)).

$$\varphi = \eta_{sens} \cdot \varphi^{Ln} \quad (1)$$

Due to the energy transfer from the Tb(III) complex, the relative quantum yield of the Eu(III) ion luminescence increases by 36% at λ_{ex} = 270 nm and 26% at λ_{ex} = 330 nm (Equations (2)–(5)) (Tables S1 and S2). A stronger luminescence of the Eu(III) complex is mostly related to the energy transfer from the ligands (η_{sens}), whereas the contribution of the quantum efficiency of the Eu^{3+} ion luminescence itself (φ^{Ln}) does not show considerable growth. The Tb(III) complex represents an additional "antenna" that provides a direct energy transfer from the Tb(III) coordination compound to the Eu^{3+} ion. Concentration changes of the Tb(III) complex also lead to changes in the emission color and provide an opportunity to control the color of the films (Figure 3b).

The 3%Eu5%Tb sample was selected to characterize luminescence of the composites at different temperatures. We chose this ratio of luminophores because it provides the optimal color visualization of temperature and almost zero concentration quenching. A relatively low content of luminophores ensures low cost of a resulting thermal sensor. It is known from the literature that luminescence quenching of Tb^{3+} ions is more strongly dependent on temperature than that of Eu^{3+} ions [3,40,41]. A simultaneous presence of Eu(III) and Tb(III) complexes in the composite films allows for a more accurate determination of temperature by evaluating the ratio of their luminescence peaks, which is not sensitive to measurement conditions.

At room temperature, the luminescence spectra of the PMMA films doped with both complexes contain the transition bands of the Eu^{3+} and Tb^{3+} ions (Figure 4). Due to the energy transfer from the Tb(III) complex to the Eu(III) complex, the excitation spectrum of the 3%Eu5%Tb film contains a more intensive excitation peak at 270 nm (Figure 4) as compared with the spectrum of the PMMA film doped with the individual Eu(III) complex. According to the CIE diagram, changing the wavelength does not lead to a considerably different perception of color (Figure 4b).

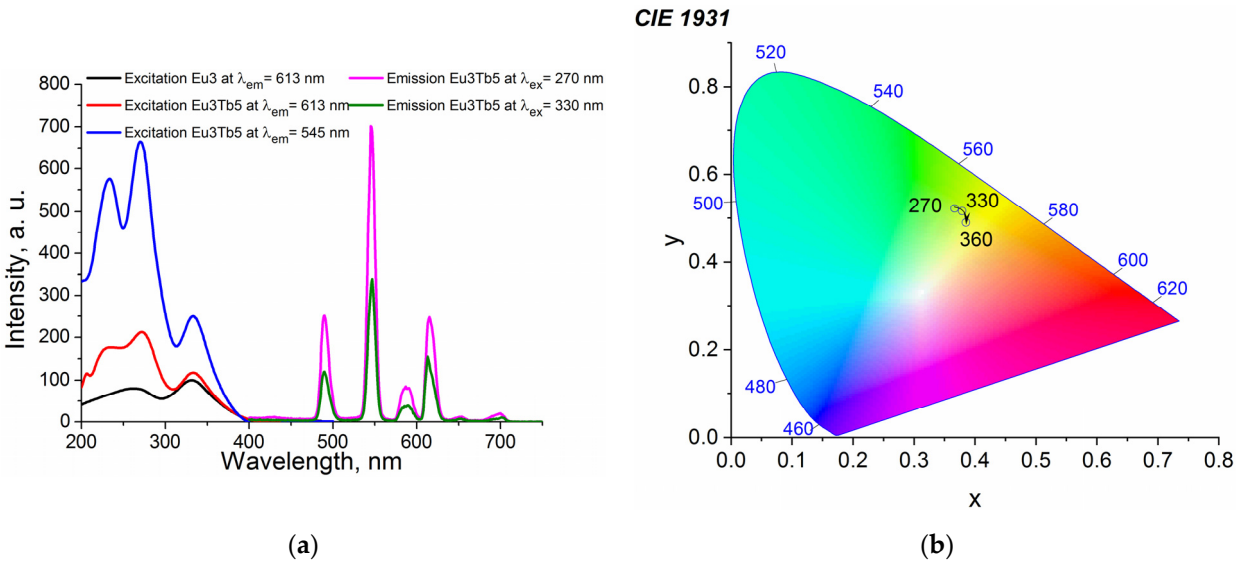

(**a**) (**b**)

Figure 4. Luminescence spectra (**a**) and the CIE diagram (**b**) of 3%Eu5%Tb at various λ_{ex}.

Figure 5a illustrates the influence of temperature on the luminescence intensity of the analyzed film in the range of 296–363 K at λ_{ex} = 330 nm and λ_{em} = 545 and 613 nm (Figure S2 at λ_{ex} = 270 nm and λ_{em} = 545 and 613 nm). Decreasing dependences of emissions from the $^5D_0 \rightarrow {}^7F_2$ (Eu(III), 613 nm) and $^5D_4 \rightarrow {}^7F_5$ (Tb(III), 545 nm) transitions are adequately described by the exponential functions with the correlation coefficients $R^2 > 0.98$.

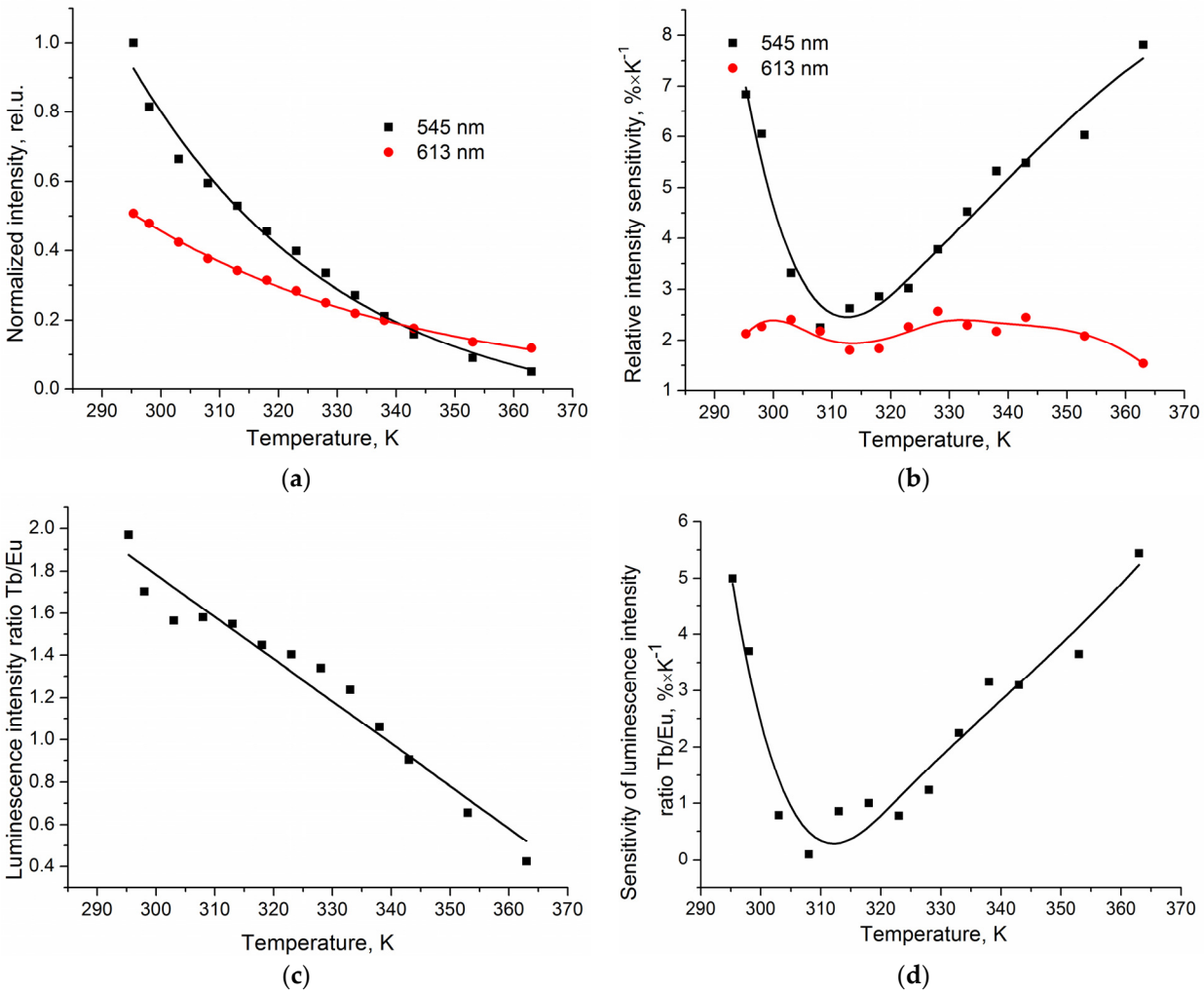

Figure 5. Temperature dependences of the normalized luminescence intensity (**a**), relative sensitivity of intensity (**b**), the ratio of luminescence intensities of the transitions $^5D_4 \rightarrow {}^7F_5$ (Tb(III), 545 nm) and $^5D_0 \rightarrow {}^7F_2$ (Eu(III), 613 nm) (**c**), and the sensitivity of the luminescence intensity ratio of the 3%Eu5%Tb composite film (**d**) at λ_{ex} = 330 nm.

The maximum value of the relative sensitivity of intensity (S_I) varies from 2.6% × K^{-1} for the $^5D_0 \rightarrow {}^7F_2$ transition (Eu(III), 613 nm) to 7.8% × K^{-1} for the $^5D_4 \rightarrow {}^7F_5$ transition (Tb(III), 545 nm) (Equation (7)).

Since luminescence of both the Tb^{3+} and Eu^{3+} ions has a specific temperature behavior, it is possible to measure temperature by the ratiometric method from the intensity ratio of the $^5D_4 \rightarrow {}^7F_5$ (Tb(III), 545 nm) and $^5D_0 \rightarrow {}^7F_2$ (Eu(III), 613 nm) transitions. The ratio of the transition intensities is almost linear ($R^2 > 0.96$) (Figure 5b and Figure S2). Therefore, the ratio of the peaks can be used to determine the surface temperature with high accuracy. The value of the maximum relative sensitivity (S_m) reaches 5.44% × K^{-1} and exceeds that of all known lanthanide-containing thermal sensors designed for measuring physiological temperatures (Table 1) [1,17].

Table 1. Comparative temperature relative sensitivity of various Ln^{3+}-based luminescent thermometers.

#	Material	Range, K	T_m, K	S_m, % × K^{-1}	Optical Parameter	Reference
1	3%Eu5%Tb	296–363	363	5.44	Two intensities	This paper
2	$Eu_{0.01}Tb_{0.99}(hfa)_3(dpbp)$	100–450	200	0.83	Two intensities	[42]
3	$Eu_{0.20}Tb_{0.80}(bpda)$	303–328	328	1.39	Two intensities	[43]
4	$Eu_{0.01}Tb_{0.99}(bdc)_{1.5}\cdot(H_2O)_2$	290–320	318	0.31	Two intensities	[44]
5	$\{Eu_{0.7}Tb_{0.3}$(d-cam)$(Himdc)_2\cdot(H_2O)_2\}_3$	100–450	450	0.11	Two intensities	[45]
6	$Eu_{0.005}Tb_{0.995}$@In(OH)(bpydc)	283–333	333	4.47	Two intensities	[46]
7	$Eu_{0.005}Tb_{0.995}$@Al(OH)(bpydc)	283–333	333	3.00	Two intensities	[46]
8	$Eu_2(qptca)(NO_3)_2(DMF)_4]\cdot[CH_3CH_2OH]_3$ perylene	293–353	293	1.28	Two intensities	[47]
9	Ln-DPA (Ln = Eu, Tb)	293–333	293	1.5	Two intensities	[48]
10	$NaGdF_4$:Yb^{3+}/Ho^{3+}/Ce^{3+}@$NaYF_4$ Yb^{3+}/Tm^{3+}	298–393	298	4.4	Two intensities	[49]
11	$NaYF_4$:Yb^{3+}/Er^{3+}@SiO_2	300–900	300	1.0	Two intensities	[50]
12	Gd_2O_3:Yb^{3+}/Er^{3+}	301–350	301	1.5	Two intensities	[51]
13	Eu^{3+}/RhB-based polymer	300–310	302	3.8	Two intensities	[52]
14	$NaGd(MoO_4)_2$:Tb^{3+}/Pr^{3+}	303–483	303	5.3	Two intensities	[53]
15	$MPr(PO_3)_4$ (M = Na, Li, K)	298–363	363	0.60	Two intensities	[54]

The films demonstrate luminescence color changes in the temperature range of 296–363 K. Therefore, they are promising colorimetric thermometers for in situ temperature measurements (Figure 6 and Figure S3). The coordinates at the CIE diagrams were calculated using the respective emission spectra from 296 K to 363 K. The luminescence color of the film changes from yellow (X = 0.411, Y = 0.514) at 296 K to red (X = 0.656, Y = 0.325) at 363 K (Figures 7 and S3).

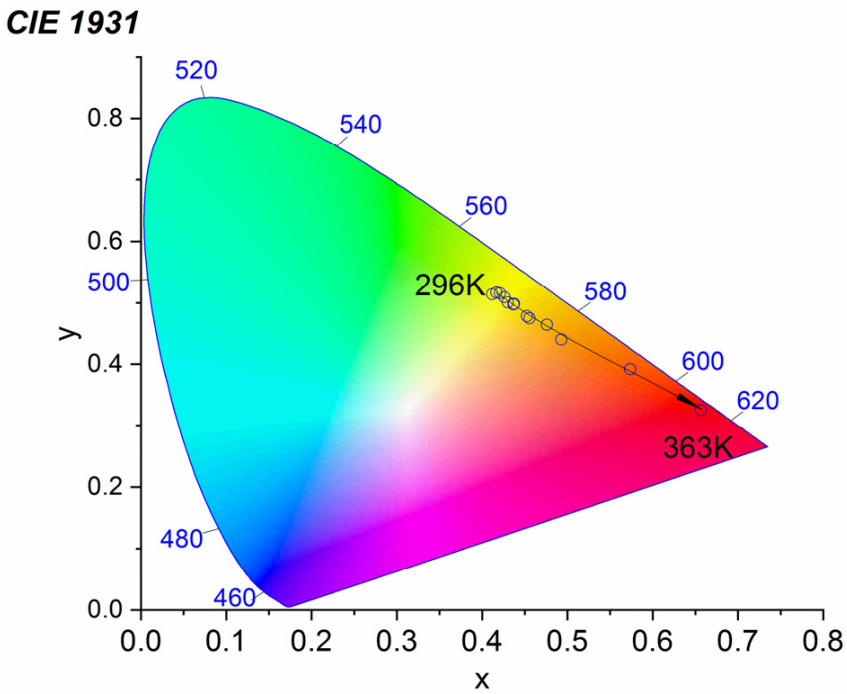

Figure 6. CIE luminescence diagram of the PMMA films doped with 3 w.% of the Eu(III) complex and 5 w.% of the Tb(III) complex (3%Eu5%Tb) at various temperatures, the excitation wavelength λ_{ex} = 330 nm.

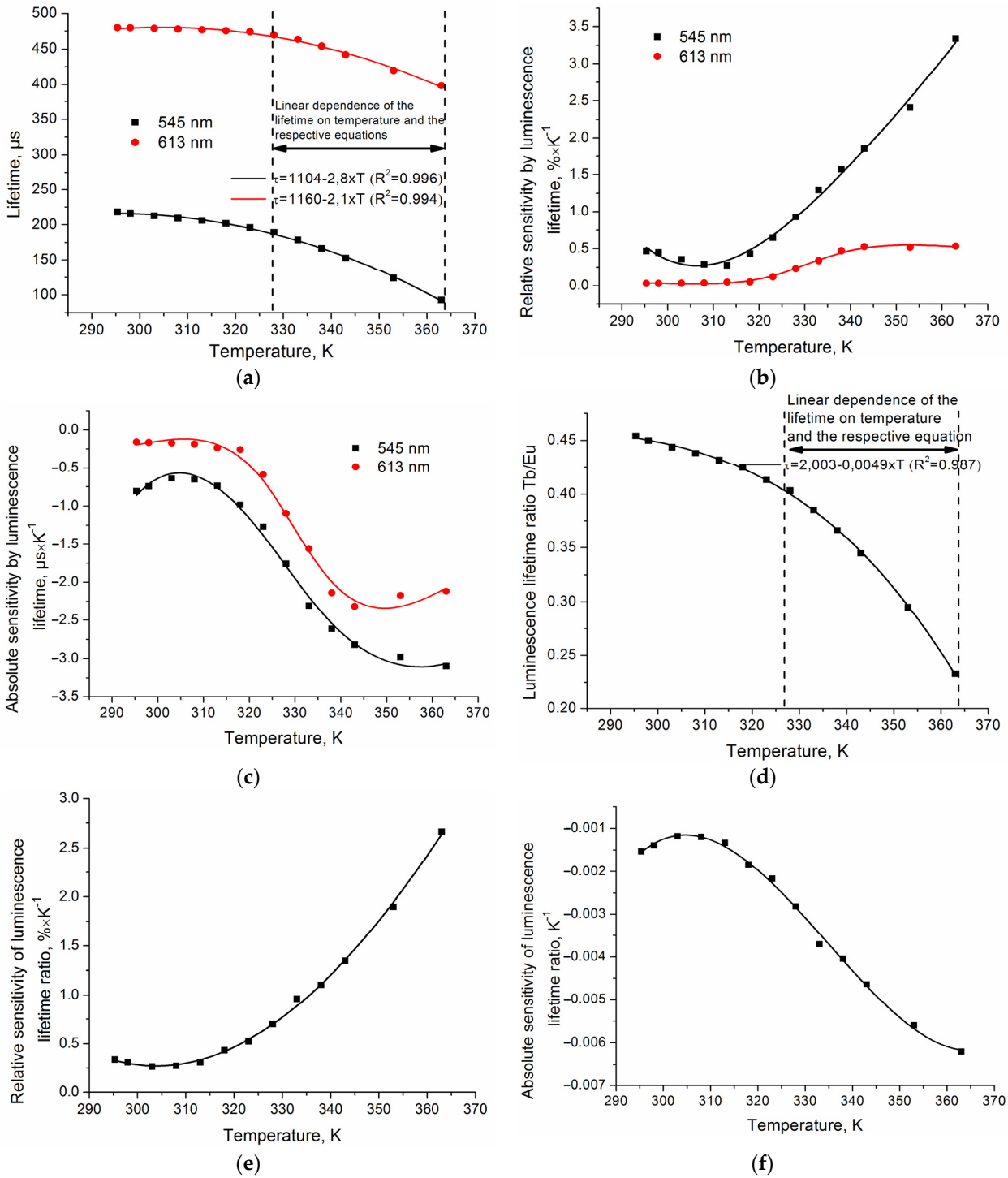

Figure 7. Temperature dependences of the luminescence lifetime (**a**), relative sensitivity of lifetime (**b**), absolute sensitivity of lifetime (**c**), the ratio of lifetimes of the $^5D_4 \rightarrow {}^7F_5$ (Tb(III), 545 nm) and $^5D_0 \rightarrow {}^7F_2$ (Eu(III), 613 nm) transitions (**d**), the relative sensitivity of the lifetime ratio (**e**), and the absolute sensitivity of the lifetime ratio (**f**) of the 3%Eu5%Tb composite film at λ_{ex} = 330 nm.

The luminescence intensity of thermally sensitive films is well-known to depend largely on the characteristics of a sample and measurement conditions [1,2]. Moreover, it is rather difficult to consider the factor of film degradation under UV radiation to avoid a significant error in temperature measurements [55–57]. Thermal sensors can also experience changes in their emission intensity when the refractive index of the medium changes (for instance, when water or other liquid is absorbed by the sensor's surface) or when chemical

or biological substances are present. The luminescence quenching time, however, does not depend on the factors mentioned above [1,2]. Therefore, this parameter is often used for more reliable and accurate temperature measurements. Figure 7a illustrates the temperature dependence of the luminescence lifetime demonstrated by the composite film samples.

In the range of 303–363 K, the luminescence lifetime of the samples decreases almost linearly as temperature increases. The slope of the temperature line between 328 K and 363 K is 2.1–2.8 μs/K (Figure 7b). The maximum relative lifetime sensitivity (Equation (7)) reaches 3.3% × K^{-1}. The curves representing the absolute sensitivity of the luminescence lifetime (Equation (6)) have similar profiles and relatively close values of 2.3–3.1 μs × K^{-1} (Figure 7).

In turn, the ratio of the luminescence lifetimes found for the $^5D_4 \rightarrow {}^7F_5$ (Tb(III), 545 nm) and $^5D_0 \rightarrow {}^7F_2$ (Eu(III), 613 nm) transitions is adequately described by a linear function (R^2>0.987) in the range of 328-363 K (Figure 7 and Figure S4). Thus, the ratio of the lifetimes of the $^5D_4 \rightarrow {}^7F_5$ (Tb(III), 545 nm) and $^5D_0 \rightarrow {}^7F_2$ (Eu(III), 613 nm) transitions allows for a high accuracy determination of a surface temperature by the ratiometric method. The slope of the temperature line representing the ratios in the range of 328–363 K is 0.0049 K^{-1}. The maximum relative lifetime sensitivity reaches 2.67% × K^{-1}. The curves representing the absolute sensitivity of the luminescence lifetime ratio have similar profiles and relatively close values of 0.0062 K^{-1}.

Stability and reversibility of thermosensor readings during heating are critical for its smooth operation. Therefore, the reversibility of intensity readings during cyclic temperature changes was examined. The luminescence intensity of the film is shown to change reversibly in the temperature range of 296–363 K (Figures 8 and S5).

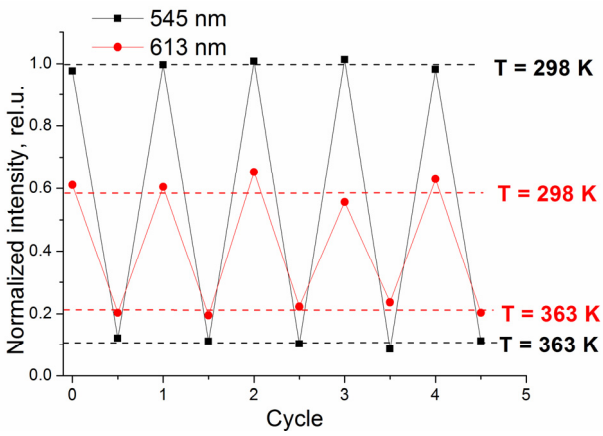

Figure 8. Reversible changes in the luminescence intensity of the 3%Eu5%Tb composite film at λ_{ex} = 330 nm during cycles of heating and cooling between 296 and 363 K.

The samples withstand five cycles of heating and cooling under irradiation at 330 nm and demonstrate a relatively small reduction in intensity (less than 2%).

Thus, these composite materials are promising components of luminescent thermometers capable of measuring temperatures in the range of 296–363 K, including the temperature of the human body.

3. Materials and Methods

3.1. Materials

$EuCl_3$*$6H_2O$ (99.9%), $TbCl_3$*$6H_2O$ (99.9%), 1,10-Phenanthroline (99%), poly(methyl methacrylate) (PMMA) (M_w~120,000 by GPC) and solvents were purchased from Sigma-Aldrich.

3.2. Characterization Techniques

CHN analysis was performed with an isotope mass spectrometer Delta V Plus Thermo Fisher Scientific. X-ray Fluorescence analysis was performed with a M4 «Tornado» Bruker

spectrometer. Absorption and transmission spectra were measured with a UV/Vis spectrophotometer Lambda-35 Perkin–Elmer. Luminescence properties were measured with a Cary Eclipse Varian spectrofluorimeter.

3.3. Synthesis of Complexes

The β-diketone (1-[4-(4-propylcyclohexyl)phenyl]-octane-1,3-dione) was prepared according to the method described in [39,58–60].

General procedure used for synthesis of the Ln(III) complexes: EtOH solution (2 mL) of $LnCl_3 \times 6H_2O$ (Ln = Tb or Eu) (0.04 mmol) was added dropwise to a stirred hot EtOH solution (10 mL) containing 1,10-Phenanthroline (0.04 mmol), β-diketone (0.12 mmol), and KOH (0.125 mmol). The resulting yellow precipitate was isolated by hot filtration, washed with hot EtOH (25 mL), and dried under vacuum. Further, the product was dissolved in toluene, filtered and the solvent was evaporated. The structural characterization results are shown in Table S3.

3.4. Preparation of PMMA–Ln(III) Films

Spin-coating of films was performed in a spin-coater (WS-650 MZ-23NPP Laurel) by deposition of 0.3 mL solution in toluene on a quartz plate [61].

3.5. Calculation of the Quantum Efficiency and Quantum Yield

To calculate the quantum efficiency of the films doped with the Eu(III) complexes, the following formula was used for Equation (2):

$$\Phi_{Ln}^{Ln} = \frac{A_{rad}}{A_{rad} + A_{nrad}} = \frac{A_{rad}}{A_{tot}} \tag{2}$$

where A_{rad} and A_{nrad} are the radiative and non-radiative rates, respectively.

The contributions to the A_{nrad} include the reverse energy transfer to the ligand [62–64], electron transfer quenching (mostly for Eu^{3+}) [64,65], and, most importantly, quenching by matrix oscillations. Luminescence of lanthanides is effectively quenched by O–H oscillations [66–69]. In addition, other oscillations of organic molecules can also contribute to A_{nrad} [69]. Non-radiative processes influence the observed luminescence lifetime ($\tau_{obs} = (A_{rad} + A_{nrad})^{-1}$). In turn, the lifetime of radiative processes can be defined as ($\tau_{rad} = A_{rad}{}^{-1}$).

Thus, we can calculate Φ^{Ln} according to the value of the observed luminescence lifetime τ_{obs} (Equation (3)).

$$\Phi_{Ln}^{Ln} = \frac{\tau_{obs}}{\tau_{Rad}} \tag{3}$$

In turn, τ_{rad} can be calculated by assuming that the energy of the $^5D_0 \rightarrow {}^7F_1$ transition and its dipole strength are constant. The resulting Equation (4) connects the form of the Eu^{3+} emission spectrum and its radiation lifetime:

$$\begin{aligned} \frac{1}{\tau_{Rad}} &= A_{MD,0} \cdot n^3 \cdot \left(\frac{I_{tot}}{I_{MD}}\right) \\ A_{MD,0} &= 14.65\ \mathrm{s}^{-1} \end{aligned} \tag{4}$$

where n is the refraction index of the medium (for a first approximation, we can use the PMMA index value)), $A_{MD,0}$ is the probability of a spontaneous emission for the $^5D_0 \rightarrow {}^7F_1$ transition in vacuum and I_{tot}/I_{MD} is the ratio of the total area of the Eu^{3+} emission to the area of the $^5D_0 \rightarrow {}^7F_1$ band. For the theoretical value of the dipole strength, it was found that $A_{MD,0} = 14.65\ \mathrm{s}^{-1}$.

The quantum yields of the PMMA–Ln(III) complexes hybrid films were calculated with Equation (5) [70]:

$$\varphi = \frac{S_u \cdot A_{st}}{A_u \cdot S_{st}} \cdot \frac{n_u^2}{n_{st}^2} \tag{5}$$

The subscripts *st* and *u* indicate the standard and unknown sample, *A*—corresponds to the absorbance of the films at the excitation wavelength λ and *S* is the integrated luminescence spectrum. The standard fluorophore for measurements was $Eu(tta)_3phen$ with φ_{std} = 53% [70].

3.6. Calculation of the Thermal Sensitivity

The absolute thermal sensitivity (S_a) is calculated as (Equation (6)) [71]:

$$S_a = \frac{\partial \Delta}{\partial T} \tag{6}$$

where Δ is luminescence lifetime or intensity.

The relative thermal sensitivity (S_r) is calculated as (Equation (7)) [71]:

$$S_r = \frac{|\partial \Delta|}{\partial T \times \Delta} \times 100\% \tag{7}$$

4. Conclusions

A spin-coating method was used to produce composite films of PMMA polymer doped with 3 w.% of the Eu(III) compound and 1–20 w.% of the Tb(III) compound. Addition of the Tb^{3+} complex increases the emission intensity of both ions due to the intermolecular energy transfer from the Tb(III) compound to the Eu(III) compound, which leads to the 36% growth of the relative luminescence quantum yield of the Eu(III) ion. We investigated the temperature sensitivity of the luminescence intensity and lifetime of the 3%Eu5%Tb films in the 296–363 K temperature range. The maximum relative sensitivity of intensity (S_I) varies from 2.6% × K^{-1} for the $^5D_0 \rightarrow {}^7F_2$ transition (613 nm) to 7.8% × K^{-1} for the $^5D_4 \rightarrow {}^7F_5$ transition (545 nm). The maximum relative sensitivity of these films reaches 5.44% × K^{-1} and exceeds that of all known lanthanide-containing thermal sensors designed for measuring physiological temperatures. Considering their luminescence color changes, the films demonstrate a significant potential as colorimetric thermal sensors for in situ temperature measurements.

Supplementary Materials: The following supporting information can be downloaded at: https://www.mdpi.com/article/10.3390/inorganics10070094/s1.

Author Contributions: This work is the collaborative development of all the authors. Conceptualization, A.A.K. and Y.G.G.; Methodology, A.A.K. and Y.G.G.; Software, A.S.K.; Validation, A.A.K., A.S.K. and Y.G.G.; Formal Analysis, A.S.K.; Investigation, A.A.K., A.S.K. and Y.G.G.; Resources, Y.G.G.; Data Curation, A.A.K. and Y.G.G.; Writing—Original Draft Preparation, A.A.K. and A.S.K.; Writing—Review and Editing, Y.G.G.; Supervision, A.A.K. and Y.G.G. All authors have read and agreed to the published version of the manuscript.

Funding: This research was funded by the Russian Science Foundation, grant number 18-13-00112.

Acknowledgments: This study was carried out using the equipment of the Center for Collective Use "Nanomaterials and Nanotechnology" of the Kazan National Research Technological University with the financial support of the Ministry of Science and Higher Education of the Russian Federation under agreement No. 075-15-2021- 699.

Conflicts of Interest: The authors declare no conflict of interests.

References

1. Wang, X.D.; Wolfbeis, O.S.; Meier, R.J. Luminescent probes and sensors for temperature. *Chem. Soc. Rev.* **2013**, *42*, 7834–7869. [CrossRef] [PubMed]
2. Brites, C.D.S.; Millán, A.; Carlos, L.D. Lanthanides in Luminescent Thermometry. In *Handbook on the Physics and Chemistry of Rare Earths*; Elsevier: Amsterdam, The Netherlands, 2016; Volume 49, pp. 339–427.
3. Brites, C.D.S.; Balabhadra, S.; Carlos, L.D. Lanthanide-Based Thermometers: At the Cutting-Edge of Luminescence Thermometry. *Adv. Opt. Mater.* **2019**, *7*, 1801239. [CrossRef]

4. Moßhammer, M.; Brodersen, K.E.; Kühl, M.; Koren, K. Nanoparticle- and microparticle-based luminescence imaging of chemical species and temperature in aquatic systems: A review. *Microchim. Acta* **2019**, *186*, 126. [CrossRef] [PubMed]
5. Hemmer, E.; Acosta-Mora, P.; Méndez-Ramos, J.; Fischer, S. Optical nanoprobes for biomedical applications: Shining a light on upconverting and near-infrared emitting nanoparticles for imaging, thermal sensing, and photodynamic therapy. *J. Mater. Chem. B* **2017**, *5*, 4365–4392. [CrossRef]
6. Brites, C.D.S.; Lima, P.P.; Silva, N.J.O.; Millán, A.; Amaral, V.S.; Palacio, F.; Carlos, L.D. Thermometry at the nanoscale. *Nanoscale* **2012**, *4*, 4799–4829. [CrossRef]
7. Dramićanin, M.D. Sensing temperature via downshifting emissions of lanthanide-doped metal oxides and salts. A review. *Methods Appl. Fluoresc.* **2016**, *4*, 042001. [CrossRef]
8. Qin, T.; Liu, B.; Zhu, K.; Luo, Z.; Huang, Y.; Pan, C.; Wang, L. Organic fluorescent thermometers: Highlights from 2013 to 2017. *TrAC—Trends Anal. Chem.* **2018**, *102*, 259–271. [CrossRef]
9. Hasegawa, Y.; Kitagawa, Y. Thermo-sensitive luminescence of lanthanide complexes, clusters, coordination polymers and metal-organic frameworks with organic photosensitizers. *J. Mater. Chem. C* **2019**, *7*, 7494–7511. [CrossRef]
10. Dai, Z.; Tian, L.; Song, B.; Ye, Z.; Liu, X.; Yuan, J. Ratiometric Time-Gated Luminescence Probe for Hydrogen Sulfide Based on Lanthanide Complexes. *Anal. Chem.* **2014**, *86*, 11883–11889. [CrossRef]
11. Zhou, J.; Xia, Z.; Bettinelli, M.; Liu, Q. Photoluminescence tuning via energy transfer in Eu-doped $Ba_2(Gd,Tb)_2Si_4O_{13}$ solid-solution phosphors. *RSC Adv.* **2015**, *6*, 2046–2054. [CrossRef]
12. Bao, G.; Wong, K.-L.; Jin, D.; Tanner, P.A. A stoichiometric terbium-europium dyad molecular thermometer: Energy transfer properties. *Light Sci. Appl.* **2018**, *7*, 1–10. [CrossRef]
13. Wang, H.; Zhao, D.; Cui, Y.; Yang, Y.; Qian, G. A Eu/Tb-mixed MOF for luminescent high-temperature sensing. *J. Solid State Chem.* **2017**, *246*, 341–345. [CrossRef]
14. Lu, H.; Meng, R.; Hao, H.; Bai, Y.; Gao, Y.; Song, Y.; Wang, Y.; Zhang, X. Stark sublevels of Er^{3+}–Yb^{3+} codoped $Gd_2(WO_4)_3$ phosphor for enhancing the sensitivity of a luminescent thermometer. *RSC Adv.* **2016**, *6*, 57667–57671. [CrossRef]
15. Lima, N.B.D.; Gonçalves, S.M.C.; Júnior, S.A.; Simas, A.M. A Comprehensive Strategy to Boost the Quantum Yield of Luminescence of Europium Complexes. *Sci. Rep.* **2013**, *3*, srep02395. [CrossRef] [PubMed]
16. Malta, O.L.; Brito, H.F.; Menezes, J.F.S.; Gonçalves e Silva, F.R.; De Mello Donegá, C.; Alves, S. Experimental and theoretical emission quantum yield in the compound Eu(thenoyltrifluoroacetonate)3.2(dibenzyl sulfoxide). *Chem. Phys. Lett.* **1998**, *282*, 233–238. [CrossRef]
17. Brites, C.D.S.; Lima, P.P.; Silva, N.J.O.; Millán, A.; Amaral, V.S.; Palacio, F.; Carlos, L.D. Lanthanide-based luminescent mo-lecular thermometers. *New J. Chem.* **2011**, *35*, 1177–1183. [CrossRef]
18. Binnemans, K. Rare-earth beta-diketonates. In *Handbook on the Physics and Chemistry of Rare Earths*; Elsevier: Amsterdam, The Netherlands, 2005; Volume 35, pp. 107–272. ISBN 9780444520289.
19. Binnemans, K. Lanthanide-Based Luminescent Hybrid Materials. *Chem. Rev.* **2009**, *109*, 4283–4374. [CrossRef]
20. Felinto Brito, H.; Manoel Loureiro Malta, O.; Claudia França Cunha Felinto, M.; Epaminondas de Sousa Teotonio, E. Luminescence Phenomena Involving Metal Enolates. In *PATAI'S Chemistry of Functional Groups*; Wiley: Hoboken, NJ, USA, 2010.
21. De Bettencourt-Dias, A. Lanthanide-based emitting materials in light-emitting diodes. *Chem. Rev.* **2007**, *22*, 2229–2241. [CrossRef]
22. Li, Y.; Bian, Y.; Yan, M.; Thapaliya, P.S.; Johns, D.; Yan, X.; Galipeau, D.; Jiang, J. Mixed (porphyrinato)(phthalocyaninato) rare-earth(III) double-decker complexes for broadband light harvesting organic solar cells. *J. Mater. Chem.* **2011**, *21*, 11131–11141. [CrossRef]
23. Lenaerts, P.; Storms, A.; Mullens, J.; D'Haen, J.; Görller-Walrand, C.; Binnemans, K.; Driesen, K. Thin Films of Highly Luminescent Lanthanide Complexes Covalently Linked to an Organic−Inorganic Hybrid Material via 2-Substituted Imidazo[4,5-*f*]-1,10-phenanthroline Groups. *Chem. Mater.* **2005**, *17*, 5194–5201. [CrossRef]
24. Li, H.R.; Lin, J.; Zhang, H.J.; Li, H.C.; Fu, L.S.; Meng, Q.G. Novel, covalently bonded hybrid materials of europium (terbium) complexes with silica. *Chem. Commun.* **2001**, *1*, 1212–1213. [CrossRef]
25. He, Y.; Liu, L.; Zhang, Z.; Fu, G.; Lü, X.; Wong, W.-K.; Jones, R.A. A tris-diketonate-Eu(III) complex with the brominated 2,2′-bpy ancillary ligand doped in PMMA for high color-purity red luminescence. *Inorg. Chem. Commun.* **2016**, *64*, 13–15. [CrossRef]
26. George, T.M.; Sajan, M.J.; Gopakumar, N.; Reddy, M.L.P. Bright red luminescence and triboluminescence from PMMA-doped polymer film materials supported by Eu 3+ -triphenylphosphine based β-diketonate and 4,5-bis(diphenylphosphino)-9,9-dimethylxanthene oxide. *J. Photochem. Photobiol. A Chem.* **2016**, *317*, 88–99. [CrossRef]
27. Li, H.; Qi, W.; Sun, H.; Li, P.; Yang, Y.; Wu, L. A novel polymerizable pigment based on surfactant-encapsulated polyoxometalates and their application in polymer coloration. *Dye Pigment.* **2008**, *79*, 105–110. [CrossRef]
28. Zhang, X.; Zhang, Z.; Liu, L.; Yu, C.; Lü, X.; Zhu, X.; Wong, W.-K.; Jones, R.A. Dual-nodal PMMA-supported Eu 3+ -containing metallopolymer with high color-purity red luminescence. *Inorg. Chem. Commun.* **2015**, *60*, 51–53. [CrossRef]
29. Xu, C.-J.; Wan, J.-T.; Li, B.-G. Monochromatic light-emitting copolymer of methyl methacrylate and Eu-complexed 5-acrylamido-1,10-phenanthroline. *Dye Pigment.* **2013**, *98*, 493–498. [CrossRef]
30. Mironov, L.Y.; Evstropiev, S. Temperature-sensitive luminescent photopolymer activated by europium β-diketonate complexes. *Opt. Eng.* **2019**, *58*, 027113. [CrossRef]

31. Knyazev, A.A.; Krupin, A.S.; Molostova, E.Y.; Romanova, K.A.; Galyametdinov, Y.G. Influence of Structural Anisotropy on Mesogenity of Eu(III) Adducts and Optical Properties of Vitrified Films Formed on their Base. *Inorg. Chem.* **2015**, *54*, 8987–8993. [CrossRef]
32. Knyazev, A.A.; Krupin, A.S.; Romanova, K.A.; Galyametdinov, Y.G. Luminescence and energy transfer in poly(N-vinylcarbazole) blends doped by a highly anisometric Eu(III) complex. *J. Coord. Chem.* **2016**, *69*, 1473–1483. [CrossRef]
33. Lapaev, D.V.; Nikiforov, V.G.; Lobkov, V.S.; Knyazev, A.A.; Krupin, A.S.; Galyametdinov, Y.G. New insights into UV laser irradiation effect on luminescent behavior of vitrified films based on mesogenic lanthanide(III) β-diketonate complexes. *J. Photochem. Photobiol. A Chem.* **2019**, *382*, 111962. [CrossRef]
34. Knyazev, A.A.; Karyakin, M.E.; Krupin, A.S.; Romanova, K.A.; Galyametdinov, Y.G. Influence of Eu(III) Complexes Structural Anisotropy on Luminescence of Doped Conjugated Polymer Blends. *Inorg. Chem.* **2017**, *56*, 6067–6075. [CrossRef] [PubMed]
35. Lapaev, D.V.; Nikiforov, V.G.; Knyazev, A.A.; Dzhabarov, V.I.; Lobkov, V.S.; Salikhov, K.M.; Galyametdinov, Y.G. Intramolecular energy transfer in mesogenic europium (III) adduct. *Opt. Spectrosc.* **2008**, *104*, 851–857. [CrossRef]
36. Romanova, K.A.; Freidzon, A.Y.; Bagaturyants, A.A.; Galyametdinov, Y.G. Ab Initio Study of Energy Transfer Pathways in Dinuclear Lanthanide Complex of Europium(III) and Terbium(III) Ions. *J. Phys. Chem. A* **2014**, *118*, 11244–11252. [CrossRef]
37. Knyazev, A.A.; Karyakin, M.E.; Heinrich, B.; Donnio, B.; Galyametdinov, Y.G. A facile approach for the creation of heteroionic lanthanidomesogens-containing uniform films with enhanced luminescence efficiency. *Dye Pigment.* **2021**, *187*, 109050. [CrossRef]
38. Knyazev, A.; Krupin, A.; Gubaidullin, A.; Galyametdinov, Y. Optical and structural characteristics of PMMA films doped with a new anisometric Eu^{III} complex. *Acta Crystallogr. Sect. B Struct. Sci. Cryst. Eng. Mater.* **2019**, *75*, 570–577. [CrossRef]
39. Knyazev, A.A.; Krupin, A.S.; Galyametdinov, Y.G. Luminescence behavior of PMMA films doped with Tb(III) and Eu(III) complexes. *J. Lumin.* **2021**, *242*, 118609. [CrossRef]
40. Liu, J.; Han, X.; Lu, Y.; Wang, S.; Zhao, D.; Li, C. Isostructural Single-and Dual-Lanthanide Metal–Organic Frameworks Based on Substituent-Group-Modifying Tetracarboxylate Ligands for Ratiometric Temperature Sensing. *Inorg. Chem.* **2021**, *60*, 4133–4143. [CrossRef] [PubMed]
41. Rocha, J.; Brites, C.D.S.; Carlos, L.D. Lanthanide Organic Framework Luminescent Thermometers. *Chem. Eur. J.* **2016**, *22*, 14782–14795. [CrossRef]
42. Hatanaka, M.; Hirai, Y.; Kitagawa, Y.; Nakanishi, T.; Hasegawa, Y.; Morokuma, K. Organic linkers control the thermosensitivity of the emission intensities from Tb(iii) and Eu(iii) in a chameleon polymer. *Chem. Sci.* **2016**, *8*, 423–429. [CrossRef]
43. Zhao, D.; Rao, X.; Yu, J.; Cui, Y.; Yang, Y.; Qian, G. Design and Synthesis of an MOF Thermometer with High Sensitivity in the Physiological Temperature Range. *Inorg. Chem.* **2015**, *54*, 11193–11199. [CrossRef]
44. Cadiau, A.; Brites, C.D.S.; Costa, P.M.F.J.; Ferreira, R.A.S.; Rocha, J.; Carlos, L.D. Ratiometric Nanothermometer Based on an Emissive Ln^{3+}-Organic Framework. *ACS Nano* **2013**, *7*, 7213–7218. [CrossRef] [PubMed]
45. Han, Y.-H.; Tian, C.-B.; Li, Q.-H.; Du, S.-W. Highly chemical and thermally stable luminescent Eu_xTb_{1-x}MOF materials for broad-range pH and temperature sensors. *J. Mater. Chem. C* **2014**, *2*, 8065–8070. [CrossRef]
46. Zhou, Y.; Yan, B.; Lei, F. Postsynthetic lanthanide functionalization of nanosized metal–organic frameworks for highly sensitive ratiometric luminescent thermometry. *Chem. Commun.* **2014**, *50*, 15235–15238. [CrossRef]
47. Cui, Y.; Song, R.; Yu, J.; Liu, M.; Wang, Z.; Wu, C.; Yang, Y.; Wang, Z.; Chen, B.; Qian, G. Dual-Emitting MOF⊃ ⋂ Dye Composite for Ratiometric Temperature Sensing. *Adv. Mater.* **2015**, *27*, 1420–1425. [CrossRef] [PubMed]
48. Rodrigues, M.; Piñol, R.; Antorrena, G.; Brites, C.D.S.; Silva, N.J.O.; Murillo, J.L.; Cases, R.; Díez, I.; Palacio, F.; Torras, N.; et al. Luminescent Thermometers: Implementing Thermometry on Silicon Surfaces Functionalized by Lanthanide-Doped Self-Assembled Polymer Monolayers. *Adv. Funct. Mater.* **2016**, *26*, 312. [CrossRef]
49. Xu, M.; Chen, D.; Huang, P.; Wan, Z.; Zhou, Y.; Ji, Z. A dual-functional upconversion core@shell nanostructure for white-light-emission and temperature sensing. *J. Mater. Chem. C* **2016**, *4*, 6516–6524. [CrossRef]
50. Geitenbeek, R.G.; Prins, P.T.; Albrecht, W.; van Blaaderen, A.; Weckhuysen, B.M.; Meijerink, A. $NaYF_4$:Er^{3+},Yb^{3+}/SiO_2 Core/Shell Upconverting Nanocrystals for Luminescence Thermometry up to 900 K. *J. Phys. Chem. C* **2017**, *121*, 3503–3510. [CrossRef]
51. Debasu, M.L.; Ananias, D.; Pastoriza-Santos, I.; Liz-Marzán, L.M.; Rocha, J.; Carlos, L.D. All-in-One Optical Heater-Thermometer Nanoplatform Operative From 300 to 2000 K Based on Er^{3+} Emission and Blackbody Radiation. *Adv. Mater.* **2013**, *25*, 4868–4874. [CrossRef]
52. Arai, S.; Takeoka, S.; Ishiwata, S.I.; Suzuki, M.; Sato, H. Facilely Fabricated Luminescent Nanoparticle Thermosensor for Real-Time Microthermography in Living Animals. *ACS Sens.* **2016**, *1*, 1222–1227. [CrossRef]
53. Gao, Y.; Huang, F.; Lin, H.; Zhou, J.; Xu, J.; Wang, Y. A Novel Optical Thermometry Strategy Based on Diverse Thermal Response from Two Intervalence Charge Transfer States. *Adv. Funct. Mater.* **2016**, *26*, 3139–3145. [CrossRef]
54. Gharouel, S.; Labrador-Páez, L.; Haro-González, P.; Horchani-Naifer, K.; Férid, M. Fluorescence intensity ratio and lifetime thermometry of praseodymium phosphates for temperature sensing. *J. Lumin.* **2018**, *201*, 372–383. [CrossRef]
55. Borisov, S.M.; Klimant, I. New luminescent oxygen-sensing and temperature-sensing materials based on gadolinium(III) and europium(III) complexes embedded in an acridone–polystyrene conjugate. *Anal. Bioanal. Chem.* **2012**, *404*, 2797–2806. [CrossRef] [PubMed]
56. Borisov, S.M.; Wolfbeis, O.S. Temperature-Sensitive Europium(III) Probes and Their Use for Simultaneous Luminescent Sensing of Temperature and Oxygen. *Anal. Chem.* **2006**, *78*, 5094–5101. [CrossRef] [PubMed]

57. Borisov, S.M.; Klimant, I. Blue LED Excitable Temperature Sensors Based on a New Europium(III) Chelate. *J. Fluoresc.* **2008**, *18*, 581–589. [CrossRef]
58. Knyazev, A.A.; Lobkov, V.S.; Galyametdinov, Y.G. Liquid-crystalline complex of Eu III β-diketonate with 5,5′-di(heptadecyl)-2,2′-bipyridine. *Russ. Chem. Bull.* **2004**, *53*, 942–943. [CrossRef]
59. Dzhabarov, V.I.; Knyazev, A.A.; Nikolaev, V.F.; Galyametdinov, Y.G. Anisotropy of the magnetic susceptibility of mesogeneous lanthanide complexes. *Russ. J. Phys. Chem. A* **2011**, *85*, 1450–1453. [CrossRef]
60. Knyazev, A.A.; Krupin, A.S.; Galyametdinov, Y.G. Anisometric Ln(III) Complexes with Efficient Near-IR Luminescence. *Inorganics* **2022**, *10*, 9. [CrossRef]
61. Knyazev, A.; Karyakin, M.; Galyametdinov, Y. Photostable anisometric lanthanide complexes as promising materials for optical applications. *Photonics* **2019**, *6*, 110. [CrossRef]
62. Bhaumik, M.L. Quenching and Temperature Dependence of Fluorescence in Rare-Earth Chelates. *J. Chem. Phys.* **1964**, *40*, 3711–3715. [CrossRef]
63. Sabbatini, N.; Guardigli, M.; Manet, I.; Ungaro, R.; Casnati, A.; Ziessel, R.; Ulrich, G.; Asfari, Z.; Lehn, J.-M. Lanthanide complexes of encapsulating ligands: Luminescent devices at the molecular level. *Pure Appl. Chem.* **1995**, *67*, 135–140. [CrossRef]
64. Prodi, L.; Maestri, M.; Balzani, V.; Lehn, J.-M.; Roth, C. Luminescence properties of cryptate europium (III) complexes incorporating heterocyclic N-oxide groups. *Chem. Phys. Lett.* **1991**, *180*, 45–50. [CrossRef]
65. Sabbatini, N.; Perathoner, S.; Lattanzi, G.; Dellonte, S.; Balzani, V. Influence of fluoride ions on the absorption and luminescence properties of the [Eu⊂2.2.1]3+ and [Tb⊂2.2.1]3+ cryptates. *J. Phys. Chem.* **1987**, *91*, 6136–6139. [CrossRef]
66. Kropp, J.L.; Windsor, M.W. Luminescence and Energy Transfer in Solutions of Rare-Earth Complexes. I. Enhancement of Fluorescence by Deuterium Substitution. *J. Chem. Phys.* **1965**, *42*, 1599–1608. [CrossRef]
67. Horrocks, W.D.W., Jr.; Sudnick, D.R. Lanthanide ion probes of structure in biology. Laser-induced luminescence decay constants provide a direct measure of the number of metal-coordinated water molecules. *J. Am. Chem. Soc.* **1979**, *101*, 334–340. [CrossRef]
68. Horrocks, W.D.W., Jr.; Sudnick, D.R. Lanthanide ion luminescence probes of the structure of biological macromolecules. *Acc. Chem. Res.* **1981**, *14*, 384–392. [CrossRef]
69. Beeby, A.; Clarkson, I.M.; Dickins, R.S.; Faulkner, S.; Parker, D.; Royle, L.; de Sousa, A.S.; Williams, J.A.G.; Woods, M. Non-radiative deactivation of the excited states of europium, terbium and ytterbium complexes by proximate energy-matched OH, NH and CH oscillators: An improved luminescence method for establishing solution hydration states. *J. Chem. Soc. Perkin Trans.* **1999**, *2*, 493–504. [CrossRef]
70. Kennedy, M.; Aubouy, L.; Jorge, A.B.; Faccini, M.; Noriega, G.; Di Lorenzo, M.; Cocca, M.; Avella, M.; Errico, M.E.; Gentile, G.; et al. Solar cell efficiency enhancement through down-shifting and up-converting layers—The ephocell project; lumi-nescent down-shifting quantum yield measurements. *Sol. Energy* **2010**, 830–833.
71. Collins, S.F.; Baxter, G.W.; Wade, S.; Sun, T.; Grattan, K.T.V.; Zhang, Z.Y.; Palmer, A.W. Comparison of fluorescence-based temperature sensor schemes: Theoretical analysis and experimental validation. *J. Appl. Phys.* **1998**, *84*, 4649–4654. [CrossRef]